On mesh-based Ewald methods: Optimal parameters for two differentiation schemes

Harry A. Stern[a] and Keith G. Calkins[b]
Department of Chemistry, University of Rochester, Rochester, New York 14607, USA

(Received 31 March 2008; accepted 1 May 2008; published online 6 June 2008)

The particle-particle particle-mesh Ewald method for the treatment of long-range electrostatics under periodic boundary conditions is reviewed. The optimal Green's function for exact (real-space differentiation), which differs from that for reciprocal-space differentiation, is given. Simple analytic formulas are given to determine the optimal Ewald screening parameter given a differentiation scheme, a real-space cutoff, a mesh spacing, and an assignment order. Simulations of liquid water are performed to examine the effect of the accuracy of the electrostatic forces on calculation of the static dielectric constant. A target dimensionless root-mean-square error of 10^{-4} is sufficient to obtain a well-converged estimate of the dielectric constant. © *2008 American Institute of Physics*. [DOI: 10.1063/1.2932253]

I. INTRODUCTION

Many molecular simulations use electrostatic models given by a set of point charges at atomic sites, and are performed under conditions of periodic boundary conditions.[1] Although there is still debate in literature,[2–4] some degree of consensus has emerged that for such a system, the Ewald sum is the most reliable method for minimizing artifacts due to finite system size.[5–7] In the past few decades several fast methods have been proposed for performing the reciprocal-space part of the Ewald sum that take advantage of the fast Fourier transform (FFT) algorithm by discretization onto a mesh.[8–13] These methods are conceptually similar, but differ in the particular way that charges are mapped onto the mesh, the way that the electrostatic potential is obtained from the mesh-based charges and the way that the potential is differentiated in order to obtain the electric field and the forces. Papers by Deserno and Holm give an excellent discussion of the subtleties of different methods.[14,15]

The present work focuses on one particular set of algorithms, variously called the particle-particle particle-mesh Ewald (P^3ME) method or smooth particle-mesh Ewald method. In this method, charges are interpolated smoothly onto mesh points. The electrostatic potential is obtained not from the "true" Coulomb Green's function but from a Green's function that is optimal (in the sense discussed below) given the particular discretization scheme. Differentiation may be performed either exactly in real space (by differentiating the weight functions used to map charges onto the mesh) or approximately in reciprocal space (by multiplying the reciprocal-space potential by $-i\mathbf{k}$).

The goals of this paper are (i) to give the optimal Green's function for exact, real-space differentiation, which differs from that for reciprocal-space differentiation, and does not seem to have appeared in literature; (ii) to give simple (fitted) formulas for the optimal Ewald screening parameter and error estimate given a differentiation scheme, a real-space cutoff, a mesh spacing, and assignment order; and (iii) to study the relation between the accuracy of the electrostatic forces and the accuracy of a calculated physical observable, the static dielectric constant. A recent paper by Ballenegger *et al.*[16] focuses on optimal Green's functions for electrostatic energies; in this paper, we focus on the accuracy of the force calculation, as that is most directly relevant for molecular dynamics simulations.

II. THEORY

Consider a neutral system of point charges q_i at locations $\mathbf{r}_i$, under periodic boundary conditions defined by primitive translation vectors $\mathbf{a}_1,\mathbf{a}_2,\mathbf{a}_3$. The energy of the system is given by

$$U=\frac{1}{2}\sum_i q_i\phi(\mathbf{r}_i), \tag{1}$$

where the electrostatic potential is given by

$$\phi(\mathbf{r}_i)=\sum_{j\ell}{}'\frac{q_j}{|\mathbf{r}_j-\mathbf{r}_i+\ell|}. \tag{2}$$

Here the sum is over all lattice vectors $\ell=n_1\mathbf{a}_1+n_2\mathbf{a}_2+n_3\mathbf{a}_3$, where n_1,n_2,n_3 are integers, and the prime denotes the omission of the $j=i$ term when $\ell=0$. This sum is only conditionally convergent and is conventionally taken to be the limit of a (roughly) spherical collection of neighboring boxes. The limit depends not only on the order in which the interactions with neighboring boxes are summed but on the medium surrounding the collection of boxes. The most common choice is to consider "tin-foil" or conducting boundary conditions, and that is the choice adopted here.

In the Ewald method, the slowly and only conditionally converging sum in Eq. (2) is evaluated by adding a screening Gaussian charge distribution of opposite sign to each point charge. The interactions between screened charges are then

[a]Electronic mail: hstern@chem.rochester.edu.
[b]Present address: Department of Mathematics, Andrews University, Berrien Springs, MI 49104. Electronic mail: calkins@andrews.edu.

 © 2008 American Institute of Physics

Author complimentary copy. Redistribution subject to AIP license or copyright, see http://jcp.aip.org/jcp/copyright.jsp

short ranged, and only neighbors within a given radius of each screened charge need to be considered. In order to recover the original potential, a canceling Gaussian charge distribution must be added as well. The potential due to this canceling Gaussian charge distribution is evaluated in Fourier space. A correction due to the interaction of a point charge with its own Gaussian screening charge must also be included. Using the Ewald method, the electrostatic potential is written as a sum of a real-space term, a self-energy term, and a reciprocal-space term, $\phi(\mathbf{r}_i)=\phi_{\text{real}}(\mathbf{r}_i)+\phi_{\text{self}}(\mathbf{r}_i)+\phi_{\text{reciprocal}}(\mathbf{r}_i)$, where

$$\phi_{\text{real}}(\mathbf{r}_i)=\sum_{j\ell}{}' q_j \frac{\text{erfc}(\eta|\mathbf{r}_i-\mathbf{r}_j+\ell|)}{|\mathbf{r}_i-\mathbf{r}_j+\ell|}, \tag{3}$$

$$\phi_{\text{self}}(\mathbf{r}_i)=-\frac{2\eta}{\sqrt{\pi}}q_i, \tag{4}$$

$$\phi_{\text{reciprocal}}(\mathbf{r}_i)=\frac{1}{V}\sum_{\mathbf{k}\neq 0} e^{i\mathbf{k}\cdot\mathbf{r}_i}\hat{G}_{\mathbf{k}}\sum_j e^{-i\mathbf{k}\cdot\mathbf{r}_j}q_j. \tag{5}$$

Here η is the width of the screening Gaussian and $V=\mathbf{a}_1\cdot(\mathbf{a}_2\times\mathbf{a}_3)$ is the volume of the basic simulation box. The reciprocal-space term is a sum over reciprocal lattice vectors $\mathbf{k}$, which are given by all linear combinations of primitive vectors for the reciprocal lattice,

$$\mathbf{b}_1=\frac{2\pi}{V}(\mathbf{a}_2\times\mathbf{a}_3), \tag{6}$$

$$\mathbf{b}_2=\frac{2\pi}{V}(\mathbf{a}_3\times\mathbf{a}_1), \tag{7}$$

$$\mathbf{b}_3=\frac{2\pi}{V}(\mathbf{a}_1\times\mathbf{a}_2). \tag{8}$$

The coefficients

$$\hat{G}_{\mathbf{k}}\equiv\frac{4\pi}{|\mathbf{k}|^2}e^{-|\mathbf{k}|^2/4\eta^2} \tag{9}$$

are the Fourier coefficients for the Green's function associated with the screening distribution (that is, the Fourier coefficients of the potential due to a charge distribution consisting of a periodic array of Gaussians centered at lattice vectors).

The basic idea behind the P^{3}M method is to discretize the charges onto a mesh and to replace the continuous Fourier transforms in Eq. (5) with discrete Fourier transforms, which can be evaluated via the FFT algorithm. The simplest way to generate a mesh is to take a simple cubic grid in "crystallographic space"—that is, to choose a number of mesh points N_1,N_2,N_3 along each primitive lattice vector and to take the set of points

$$\mathbf{r}_{\mathbf{n}}\equiv\frac{n_1}{N_1}\mathbf{a}_1+\frac{n_2}{N_2}\mathbf{a}_2+\frac{n_3}{N_3}\mathbf{a}_3. \tag{10}$$

Here $\mathbf{n}=(n_1,n_2,n_3)$ is a triplet of integers, each one chosen from 0 to N_1-1,N_2-1,N_3-1, respectively. Associated with the lattice of mesh points is a (finite) reciprocal lattice,

$$\mathbf{k}_{\mathbf{n}}\equiv n_1\mathbf{b}_1+n_2\mathbf{b}_2+n_3\mathbf{b}_3. \tag{11}$$

The charges at each mesh point $q_{\mathbf{r}_{\mathbf{n}}}$ are computed from an assignment function $W(\mathbf{r})$:

$$q_{\mathbf{r}_{\mathbf{n}}}=\sum_i q_i W(\mathbf{r}_{\mathbf{n}}-\mathbf{r}_i). \tag{12}$$

The particular form of the assignment function is discussed below; for now, it is simply assumed that it is even and differentiable.

Once the charges are assigned to the real-space mesh, the Fourier coefficients of the mesh-based charge density

$$\hat{\rho}_{\mathbf{k}_{\mathbf{n}}}=\frac{1}{V}\sum_{\mathbf{r}_{\mathbf{n}}} e^{-i\mathbf{k}_{\mathbf{n}}\cdot\mathbf{r}_{\mathbf{n}}}q_{\mathbf{r}_{\mathbf{n}}} \tag{13}$$

may be computed via the FFT algorithm. The Fourier coefficients of the mesh-based potential are then given by multiplying those of the charge density by those of the Green's function. A key idea in the P^{3}M method is to replace the Fourier coefficients of the actual screened Coulomb Green's function $\hat{G}_{\mathbf{k}}=(4\pi/|\mathbf{k}|^2)e^{-|\mathbf{k}|^2/4\eta^2}$ with different coefficients $\hat{G}'_{\mathbf{k}_n}$, which are chosen to minimize the error resulting from discretization,[8,14] so that

$$\hat{\phi}_{\mathbf{k}_{\mathbf{n}}}=\sum_{\mathbf{k}_{\mathbf{n}}\neq 0}\hat{G}'_{\mathbf{k}_{\mathbf{n}}}\hat{\rho}_{\mathbf{k}_{\mathbf{n}}}. \tag{14}$$

The potential on the real-space mesh is then computed from a reverse FFT:

$$\phi_{\mathbf{r}_{\mathbf{n}}}=\sum_{\mathbf{k}_{\mathbf{n}}} e^{i\mathbf{k}_{\mathbf{n}}\cdot\mathbf{r}_{\mathbf{n}}}\hat{\phi}_{\mathbf{k}_{\mathbf{n}}}. \tag{15}$$

Finally, the mesh-based potential is interpolated back to the locations of the actual charges using the same assignment function:

$$\phi(\mathbf{r}_i)=\sum_{\mathbf{r}_{\mathbf{n}}}\phi_{\mathbf{r}_{\mathbf{n}}}W(\mathbf{r}_i-\mathbf{r}_{\mathbf{n}}). \tag{16}$$

The P^{3}M reciprocal-space potential is therefore

$$\phi_{\text{P}^3\text{M}}(\mathbf{r}_i)=\sum_{\mathbf{r}'_{\mathbf{n}}}W(\mathbf{r}_i-\mathbf{r}'_{\mathbf{n}})\frac{1}{V}\sum_{\mathbf{k}_{\mathbf{n}}\neq 0}e^{i\mathbf{k}_{\mathbf{n}}\cdot\mathbf{r}'_{\mathbf{n}}}\hat{G}'_{\mathbf{k}_{\mathbf{n}}}\sum_{\mathbf{r}_{\mathbf{n}}}e^{-i\mathbf{k}_{\mathbf{n}}\cdot\mathbf{r}_{\mathbf{n}}}\sum_j \times W(\mathbf{r}_{\mathbf{n}}-\mathbf{r}_j)q_j, \tag{17}$$

where $\hat{G}'_{\mathbf{k}_n}$ remains to be determined.

In order to determine the forces on the particles, the potential must be differentiated to obtain the electric field. There are several methods by which this can be done. This paper considers two: exact differentiation in real space using the gradient of the assignment function, which gives

$$\mathbf{E}_{\text{P}^3\text{M}}(\mathbf{r}_i)=\sum_{\mathbf{r}'_{\mathbf{n}}}-\nabla W(\mathbf{r}_i-\mathbf{r}'_{\mathbf{n}})\frac{1}{V}\sum_{\mathbf{k}_{\mathbf{n}}\neq 0}e^{i\mathbf{k}_{\mathbf{n}}\cdot\mathbf{r}'_{\mathbf{n}}}\hat{G}'_{\mathbf{k}_{\mathbf{n}}} \times\sum_{\mathbf{r}_{\mathbf{n}}}e^{-i\mathbf{k}_{\mathbf{n}}\cdot\mathbf{r}_{\mathbf{n}}}\sum_j W(\mathbf{r}_{\mathbf{n}}-\mathbf{r}_j)q_j, \tag{18}$$

and approximate differentiation on the reciprocal-space mesh by multiplying the potential by $i\mathbf{k}_{\mathbf{n}}$, which gives

Author complimentary copy. Redistribution subject to AIP license or copyright, see http://jcp.aip.org/jcp/copyright.jsp

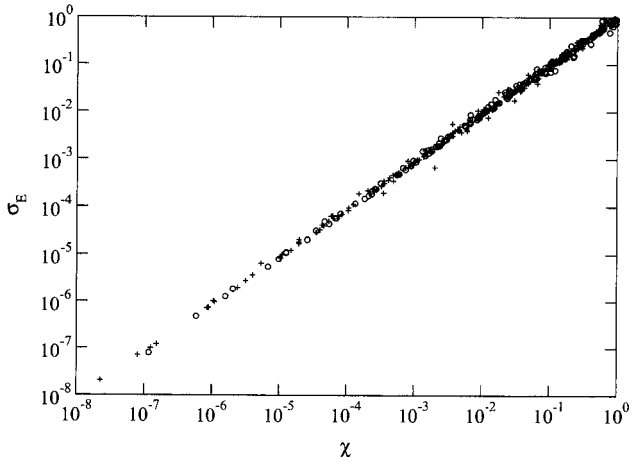

FIG. 1. Comparison between analytical estimate for the dimensionless rms error in the reciprocal-space contribution to the electric field χ with the numerical rms error for a randomly distributed unit source charge and target location in a cubic box of unit volume, σ_E. Circles, real-space differentiation; crosses, reciprocal-space differentiation. P^{3}M calculations were performed with grid spacings ranging from 0.01 to 0.1, assignment orders from 2 to 5, and screening parameters from 4 to 32.

$$\mathbf{E}_{\mathrm{P^3M}}(\mathbf{r}_i) = \sum_{\mathbf{r}'_\mathbf{n}} W(\mathbf{r}_i - \mathbf{r}'_\mathbf{n}) \frac{1}{V} \sum_{\mathbf{k_n} \neq 0} e^{i\mathbf{k_n}\cdot\mathbf{r}'_\mathbf{n}} \times (-i\mathbf{k_n}) \hat{G}'_{\mathbf{k_n}} \sum_{\mathbf{r_n}} e^{-i\mathbf{k_n}\cdot\mathbf{r_n}} \sum_j W(\mathbf{r_n} - \mathbf{r}_j) q_j. \quad (19)$$

If real-space differentiation is performed, only one reverse FFT needs to be done. If differentiation on the reciprocal-space mesh is used, a total of four reverse FFTs is needed: one for the potential and one for each component of the field.

As mentioned above, the coefficients of the reciprocal-space mesh-based Green's function $\hat{G}_{\mathbf{k_n}}$ are chosen to minimize the error in the calculated electric field due to discretization. One estimate for this discretization error is the square of the error in the field due to a Gaussian distribution of unit charge, integrated over all positions within the primary unit cell, and all positions of the distribution:[8]

$$\chi^2_{\mathrm{P^3M}} \equiv V^{-2/3} \int_V \int_V |\mathbf{E}_{\mathrm{P^3M}}(\mathbf{r}_1, \mathbf{r}_2) - \mathbf{E}_{\mathrm{reciprocal}}(\mathbf{r}_1, \mathbf{r}_2)|^2 d^3 r_1 d^3 r_2. \quad (20)$$

Here $\mathbf{E}_{\mathrm{P^3M}}(\mathbf{r}_1, \mathbf{r}_2)$ and $\mathbf{E}_{\mathrm{reciprocal}}(\mathbf{r}_1, \mathbf{r}_2)$ denote the electric field at $\mathbf{r}_1$ due to a Gaussian distribution of total unit charge centered at $\mathbf{r}_2$, calculated with P^{3}M and with the ordinary Ewald reciprocal-space sum, respectively. The factor of $V^{-2/3}$ is chosen to make $\chi_{\mathrm{P^3M}}$ dimensionless. Equation (20) is related to the root-mean-square (rms) error in the forces for a system of N charges q_i by[15]

$$\Delta F_{\mathrm{P^3M}} \approx \left[\sum_{i=1}^{N} q_i^2 \right] N^{-1/2} V^{-2/3} \chi_{\mathrm{P^3M}}.$$

For differentiation in real space, minimizing Eq. (20) with respect to $\hat{G}'_{\mathbf{k_n}}$ yields

$$\hat{G}'_{\mathbf{k_n}} = \frac{\Sigma_\mathbf{M} \hat{U}^2_{\mathbf{k_{n+M}}} \hat{G}_{\mathbf{k_{n+M}}} |\mathbf{k_{n+M}}|^2}{[\Sigma_\mathbf{M} \hat{U}^2_{\mathbf{k_{n+M}}}][\Sigma_\mathbf{M} \hat{U}^2_{\mathbf{k_{n+M}}} |\mathbf{k_{n+M}}|^2]}. \quad (21)$$

For differentiation on the reciprocal-space mesh, a different expression is obtained,

$$\hat{G}'_{\mathbf{k_n}} = \frac{\Sigma_\mathbf{M} \hat{U}^2_{\mathbf{k_{n+M}}} \hat{G}_{\mathbf{k_{n+M}}} \mathbf{k_n} \cdot \mathbf{k_{n+M}}}{[\Sigma_\mathbf{M} \hat{U}^2_{\mathbf{k_{n+M}}}]^2 |\mathbf{k_n}|^2}. \quad (22)$$

Equations (21) and (22) are derived in the Appendix. In these equations,

$$\hat{U}_\mathbf{k} \equiv \frac{N_1 N_2 N_3}{V} \hat{W}_\mathbf{k}, \quad (23)$$

where

$$\hat{W}_\mathbf{k} = \int_V e^{-i\mathbf{k}\cdot\mathbf{r}} W(\mathbf{r}) d^3 r \quad (24)$$

are the Fourier coefficients of the assignment function. Since the assignment function is even, the coefficients are real and $\hat{W}_\mathbf{k} = \hat{W}_{-\mathbf{k}}$. $\mathbf{M}$ is a triplet of multiples of the number of grid-points in each dimension; that is,

$$\mathbf{M} \equiv (m_1 N_1, m_2 N_2, m_3 N_3), \quad (25)$$

where m_1, m_2, m_3 are integers. The sums are over all such triplets, and

$$\mathbf{k_{n+M}} \equiv (n_1 + m_1 N_1)\mathbf{b}_1 + (n_2 + m_2 N_2)\mathbf{b}_2 + (n_3 + m_3 N_3)\mathbf{b}_3. \quad (26)$$

In practice, only a few triplets $\mathbf{M}$ need to be included in the sum for each $\mathbf{n}$, since $\hat{G}_\mathbf{k}$ and $\hat{U}_\mathbf{k}$ decrease rapidly as $|\mathbf{k}|$ becomes large.

It is stressed that the Green's function coefficients yielding the best accuracy in the forces will depend on the method of differentiation. Equation (21) gives the best Green's function coefficients in the case that differentiation is performed

TABLE I. For real-space differentiation: optimal Ewald screening parameter η given in terms of the real-space cutoff r_c and grid spacing s by the formula $\eta = \exp[a_1 r_c^2 + a_2 (\ln s)^2 + a_3 r_c (\ln s) + a_4 r_c + a_5 s + a_6]$ for several assignment orders and unit box length.

Assignment Order	a_1	a_2	a_3	a_4	a_5	a_6
2	6.551	−0.031	0.209	−6.371	−0.441	2.143
3	6.012	−0.042	0.359	−5.355	−0.587	1.978
4	5.551	−0.054	0.460	−4.595	−0.728	1.694
5	5.249	−0.061	0.513	−4.113	−0.824	1.477

Author complimentary copy. Redistribution subject to AIP license or copyright, see http://jcp.aip.org/jcp/copyright.jsp

TABLE II. For real-space differentiation: dimensionless rms error χ for optimal η given in terms of the real-space cutoff r_c and grid spacing s by the formula $\eta=\exp[a_1 r_c^2+a_2(\ln s)^2+a_3 r_c(\ln s)+a_4 r_c+a_5 s+a_6]$ for several assignment orders and unit box length.

Assignment order	a_1	a_2	a_3	a_4	a_5	a_6
2	9.625	−0.027	0.104	−9.976	0.589	3.596
3	18.590	−0.010	0.123	−18.494	1.611	6.161
4	25.453	−0.010	0.157	−26.037	2.525	9.045
5	31.248	−0.053	0.700	−31.014	2.998	11.187

in real space, while Eq. (22) gives the best Green's function coefficients in the case that differentiation is performed on the reciprocal-space mesh.

The mean-square error for real-space differentiation is

$$\chi_{\mathrm{P^3M}}^2 V^{2/3} = \left(\sum_{\mathbf{k}\neq 0} \hat{G}_{\mathbf{k}}^2 |\mathbf{k}|^2\right) - \sum_{\mathbf{n}} \left(\frac{[\Sigma_{\mathbf{M}} \hat{U}^2_{\mathbf{k_{n+M}}} \hat{G}_{\mathbf{k_{n+M}}} |\mathbf{k_{n+M}}|^2]^2}{[\Sigma_{\mathbf{M}} \hat{U}^2_{\mathbf{k_{n+M}}}][\Sigma_{\mathbf{M}} \hat{U}^2_{\mathbf{k_{n+M}}} |\mathbf{k_{n+M}}|^2]} \right), \quad (27)$$

and for reciprocal-space differentiation is

$$\chi_{\mathrm{P^3M}}^2 V^{2/3} = \left(\sum_{\mathbf{k}\neq 0} \hat{G}_{\mathbf{k}}^2 |\mathbf{k}|^2\right) - \sum_{\mathbf{n}} \left(\frac{[\Sigma_{\mathbf{M}} \hat{U}^2_{\mathbf{k_{n+M}}} \hat{G}_{\mathbf{k_{n+M}}} \mathbf{k}_n \cdot \mathbf{k_{n+M}}]^2}{[\Sigma_{\mathbf{M}} \hat{U}^2_{\mathbf{k_{n+M}}}]^2 |\mathbf{k_n}|^2} \right), \quad (28)$$

in each case using the optimal Green's function coefficients for that method of differentiation.

At this point it is still necessary to specify the form of the assignment function $W(\mathbf{r})$, which gives the fraction of charge assigned to a grid point at a displacement $\mathbf{r}$ from a charge. We use here the set of assignment functions given by Hockney and Eastwood.[8,14] To construct $W(\mathbf{r})$ for arbitrary periodic boundary conditions, an assignment function $w(s)$ is first considered for a one-dimensional mesh with unit spacing between mesh points. A p-order assignment function (that is, an assignment function that assigns a charge to p mesh points) may be constructed from a p-fold convolution of the indicator function on the interval $[-\frac{1}{2},\frac{1}{2}]$:

$$w_p(s) = \left(\underbrace{\mathbf{1}_{[-1/2,1/2]} \star \cdots \star \mathbf{1}_{[-1/2,1/2]}}_{p\text{-fold convolution}} \right)(s), \quad (29)$$

where

$$\mathbf{1}_{[-1/2,1/2]}(s) = \begin{cases} 1 & \text{if } -\frac{1}{2} \leqslant s \leqslant \frac{1}{2} \\ 0 & \text{otherwise.} \end{cases} \quad (30)$$

The Fourier transform of this assignment function is

$$\hat{w}_p(\kappa) = \int w_p(s) e^{-i\kappa s} ds \quad (31)$$

$$= \left[\frac{\sin(\kappa/2)}{\kappa/2} \right]^p. \quad (32)$$

The actual assignment function $W(\mathbf{r})$ may then be written as a product of the displacement along each lattice vector, scaled by the number of gridpoints:

$$W(\mathbf{r}) = w(s_1) w(s_2) w(s_3), \quad (33)$$

where

$$\mathbf{r} = \frac{s_1}{N_1}\mathbf{a}_1 + \frac{s_2}{N_2}\mathbf{a}_2 + \frac{s_3}{N_3}\mathbf{a}_3. \quad (34)$$

Here s_1, s_2, s_3 are dimensionless coordinates ranging from 0 to N_1, N_2, N_3. Therefore,

$$\hat{U}(\mathbf{k_n}) = \frac{N_1 N_2 N_3}{V} \int_V e^{-2\pi i n_1 s_1/N_1} e^{-2\pi i n_2 s_2/N_2} e^{-2\pi i n_3 s_3/N_3} \times w(s_1) w(s_2) w(s_3) d^3 r \quad (35)$$

$$= \left[\frac{\sin(\pi n_1/N_1)}{\pi n_1/N_1} \right]^p \left[\frac{\sin(\pi n_2/N_2)}{\pi n_2/N_2} \right]^p \left[\frac{\sin(\pi n_3/N_3)}{\pi n_3/N_3} \right]^p. \quad (36)$$

III. NUMERICAL RESULTS

The expressions for the rms error for both differentiation methods, Eqs. (27) and (28), were checked by comparing with numerical calculations. Parameters were chosen such that the accuracy of the calculations would vary over several orders of magnitude. Results are shown in Fig. 1; close agreement between the analytical expression and numerical calculation is obtained.

An estimate for the rms error in the forces due to the real-space part of the Ewald sum due to Kolafa and Perram[17] is

$$\Delta F_{\text{real space}} \approx \left[\sum_{i=1}^{N} q_i^2 \right] N^{-1/2} V^{-2/3} \chi_{\text{real space}},$$

where

$$\chi_{\text{real space}} = \frac{2}{\sqrt{r_c V^{1/3}}} e^{-\eta^2 r_c^2}.$$

The dimensionless estimate $\chi_{\text{real space}}$ may be added to that for the reciprocal-space forces in order to obtain a total error estimate. The total estimate may then be minimized with respect to the screening parameter η in order to obtain an optimal value. This was performed for several different values of the real-space cutoff r_c, grid spacing s, and assignment

Author complimentary copy. Redistribution subject to AIP license or copyright, see http://jcp.aip.org/jcp/copyright.jsp

TABLE III. For reciprocal-space differentiation: optimal Ewald screening parameter η given in terms of the real-space cutoff r_c and grid spacing s by the formula $\eta=\exp[a_1 r_c^2+a_2(\ln s)^2+a_3 r_c(\ln s)+a_4 r_c+a_5 s+a_6]$ for several assignment orders and unit box length.

Assignment order	a_1	a_2	a_3	a_4	a_5	a_6
2	5.902	−0.043	0.365	−5.238	−0.603	1.875
3	5.434	−0.055	0.473	−4.461	−0.745	1.612
4	5.101	−0.064	0.540	−3.917	−0.852	1.376
5	4.815	−0.069	0.576	−3.529	−0.925	1.200

order. The optimal screening parameters and errors using them were fitted to a simple analytical expression, as shown in Tables I–IV. These expressions allow one to obtain the optimal screening parameter and associated error for a given real-space cutoff, grid spacing, and assignment order. The deviation between the analytic expressions and actual values was small (on the order of a few percent) for the range of cutoffs, spacings, and assignment orders.

In order to determine the relationship between the accuracy of the electrostatic forces, as given by the dimensionless mean-square error described above, and a physical observable which is fairly demanding to calculate (the static dielectric constant), several simulations of liquid water were performed using the simple point charge/extended water model.[18] The system consisted of 216, 343, or 512 water molecules, under conditions of constant volume, in a cubic box with size chosen such that the density was 0.997 $\mathrm{g/cm^3}$. Temperature was maintained at 298 K using intermittent resampling of velocities from the Boltzmann distribution. Periodic boundary conditions were used with Lennard-Jones forces and real-space electrostatic forces smoothly truncated at 9 Å, fourth-order assignment, and grid spacings varying from one-hundredth to one-tenth of the box size. For each grid spacing, 18 independent simulations were run, each consisting of 10^6 2 fs timesteps for a total duration of 36 ns. The dielectric constant was calculated from the mean-square value of the total system dipole moment,

$$\epsilon = 1 + \frac{4\pi}{3Vk_{\mathrm{B}}T}\langle \mathbf{M}^2 \rangle.$$

Results are shown in Fig. 2. They indicate that a reasonable target value for the dimensionless rms error is around 10^{-4} independent of system size.

IV. CONCLUSIONS

In this paper we derived the optimal Green's function for the particle-particle $\mathrm{P^3ME}$ method using exact, real-space differentiation, which differs from that for reciprocal-space differentiation. We determined optimal values for the Ewald screening parameter (for both methods of differentiation) for a range of real-space cutoffs, grid spacings, and assignment orders. These and the associated dimensionless rms errors in the force were fitted to simple analytical forms. These expressions should be a practical tool for choosing appropriate parameters for the Ewald calculation, given a particular system size and target accuracy. Given that the static dielectric constant of water exhibits strong dependence on the treatment of long-range electrostatic forces,[1,19] it is a good property for determining an appropriate target accuracy for the $\mathrm{P^3M}$ calculation. The present simulations show that this target accuracy as given by the dimensionless rms error should be around 10^{-4}, independent of system size. It should be noted that a target accuracy, which leads to good convergence of the static dielectric constant for water, should be more than accurate enough for large-scale simulations of biological molecules,[20–22] which are subject to many other sources of error, most notably due to the potential energy function.

APPENDIX: ESTIMATES OF THE $\mathrm{P^3M}$ DISCRETIZATION ERROR FOR REAL-SPACE AND RECIPROCAL-SPACE DIFFERENTIATION

The estimate for the discretization error of the $\mathrm{P^3M}$ method is

$$\chi^2_{\mathrm{P^3M}} \equiv V^{-2/3}\int_V \int_V |\mathbf{E}_{\mathrm{P^3M}}(\mathbf{r}_1,\mathbf{r}_2) - \mathbf{E}_{\mathrm{reciprocal}}(\mathbf{r}_1,\mathbf{r}_2)|^2 d^3r_1 d^3r_2. \quad \text{(A1)}$$

Here $\mathbf{E}_{\mathrm{P^3M}}(\mathbf{r}_1,\mathbf{r}_2)$ and $\mathbf{E}_{\mathrm{reciprocal}}(\mathbf{r}_1,\mathbf{r}_2)$ denote the electric field at $\mathbf{r}_1$ due to a Gaussian distribution of total unit charge centered at $\mathbf{r}_2$, calculated with $\mathrm{P^3M}$ with the ordinary Ewald reciprocal-space sum, respectively. By Parseval's theorem,

TABLE IV. For reciprocal-space differentiation: dimensionless rms error χ for optimal η given in terms of the real-space cutoff r_c and grid spacing s by the formula $\eta=\exp[a_1 r_c^2+a_2(\ln s)^2+a_3 r_c(\ln s)+a_4 r_c+a_5 s+a_6]$ for several assignment orders and unit box length.

Assignment order	a_1	a_2	a_3	a_4	a_5	a_6
2	17.483	−0.034	0.344	−16.878	1.314	5.680
3	24.524	−0.035	0.357	−24.508	2.213	8.453
4	30.505	−0.072	0.806	−29.898	2.752	10.702
5	35.825	−0.137	1.573	−33.543	2.963	12.329

Author complimentary copy. Redistribution subject to AIP license or copyright, see http://jcp.aip.org/jcp/copyright.jsp

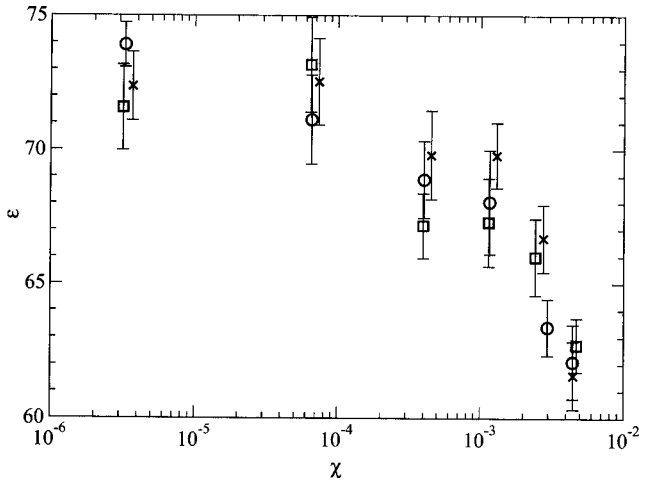

FIG. 2. Dielectric constant for liquid water ϵ as a function of the dimensionless rms error in the force, χ. Circles, 216 water molecules; squares, 343 water molecules; crosses, 512 water molecules. Error bars are the standard error of the mean taken from block averaging.

$$\chi^2_{\mathrm{P^3M}} = V^{-8/3}\sum_{\mathbf{k}_1}\sum_{\mathbf{k}_2}|\hat{\mathbf{E}}_{\mathrm{P^3M}}(\mathbf{k}_1,\mathbf{k}_2) - \hat{\mathbf{E}}_{\mathrm{reciprocal}}(\mathbf{k}_1,\mathbf{k}_2)|^2, \tag{A2}$$

where

$$\hat{\mathbf{E}}_{\mathrm{P^3M,reciprocal}}(\mathbf{k}_1,\mathbf{k}_2) \equiv \int_V\int_V \mathbf{E}_{\mathrm{P^3M,reciprocal}} \times(\mathbf{r}_1,\mathbf{r}_2)e^{-i\mathbf{k}_1\cdot\mathbf{r}_1}e^{-i\mathbf{k}_2\cdot\mathbf{r}_2}d^3r_1d^3r_2, \tag{A3}$$

and the sums are over all reciprocal lattice vectors. The ordinary Ewald reciprocal-space field is given by

$$\mathbf{E}_{\mathrm{reciprocal}}(\mathbf{r}_1,\mathbf{r}_2) = \frac{1}{V}\sum_{\mathbf{k}\neq 0}(-i\mathbf{k})\hat{G}_{\mathbf{k}}e^{i\mathbf{k}\cdot(\mathbf{r}_1-\mathbf{r}_2)}, \tag{A4}$$

where $\hat{G}_{\mathbf{k}} \equiv (4\pi/|\mathbf{k}|^2)e^{-|\mathbf{k}|^2/4\eta^2}$.

For differentiation in real space using the gradient of the assignment function,

$$\mathbf{E}_{\mathrm{P^3M}}(\mathbf{r}_1,\mathbf{r}_2) = \sum_{\mathbf{r}'_{\mathbf{n}}} -\nabla W(\mathbf{r}_1-\mathbf{r}'_{\mathbf{n}}) \times\frac{1}{V}\sum_{\mathbf{k}_{\mathbf{n}}\neq 0} e^{i\mathbf{k}_{\mathbf{n}}\cdot\mathbf{r}'_{\mathbf{n}}}\hat{G}'_{\mathbf{k}_{\mathbf{n}}}\sum_{\mathbf{r}_{\mathbf{n}}} e^{-i\mathbf{k}_{\mathbf{n}}\cdot\mathbf{r}_{\mathbf{n}}}W(\mathbf{r}_{\mathbf{n}}-\mathbf{r}_2). \tag{A5}$$

Therefore,

$$\begin{aligned}
\hat{\mathbf{E}}_{\mathrm{P^3M}}(\mathbf{k}_1,\mathbf{k}_2) &= -\frac{1}{V}\sum_{\mathbf{r}'_{\mathbf{n}}}\left[\int_V \nabla W(\mathbf{r}_1-\mathbf{r}'_{\mathbf{n}})e^{-i\mathbf{k}_1\cdot\mathbf{r}_1}d^3r_1\right]\sum_{\mathbf{k}_{\mathbf{n}}\neq 0} e^{i\mathbf{k}_{\mathbf{n}}\cdot\mathbf{r}'_{\mathbf{n}}}\hat{G}'_{\mathbf{k}_{\mathbf{n}}}\sum_{\mathbf{r}_{\mathbf{n}}} e^{-i\mathbf{k}_{\mathbf{n}}\cdot\mathbf{r}_{\mathbf{n}}}\times\left[\int_V W(\mathbf{r}_{\mathbf{n}}-\mathbf{r}_2)e^{-i\mathbf{k}_2\cdot\mathbf{r}_2}d^3r_2\right] \\
&= -\frac{1}{V}\sum_{\mathbf{r}'_{\mathbf{n}}}[i\mathbf{k}_1\hat{W}_{\mathbf{k}_1}e^{-i\mathbf{k}_1\cdot\mathbf{r}'_{\mathbf{n}}}]\sum_{\mathbf{k}_{\mathbf{n}}\neq 0} e^{i\mathbf{k}_{\mathbf{n}}\cdot\mathbf{r}'_{\mathbf{n}}}\hat{G}'_{\mathbf{k}_{\mathbf{n}}}\sum_{\mathbf{r}_{\mathbf{n}}} e^{-i\mathbf{k}_{\mathbf{n}}\cdot\mathbf{r}_{\mathbf{n}}}[\hat{W}_{\mathbf{k}_2}e^{-i\mathbf{k}_2\cdot\mathbf{r}_{\mathbf{n}}}] \\
&= -\frac{1}{V}i\mathbf{k}_1\hat{W}_{\mathbf{k}_1}\hat{W}_{\mathbf{k}_2}\sum_{\mathbf{k}_{\mathbf{n}}\neq 0}\hat{G}'_{\mathbf{k}_{\mathbf{n}}}\left[\sum_{\mathbf{r}'_{\mathbf{n}}} e^{-i(\mathbf{k}_1-\mathbf{k}_{\mathbf{n}})\cdot\mathbf{r}'_{\mathbf{n}}}\right]\left[\sum_{\mathbf{r}_{\mathbf{n}}} e^{-i(\mathbf{k}_{\mathbf{n}}+\mathbf{k}_2)\cdot\mathbf{r}_{\mathbf{n}}}\right] \\
&= -Vi\mathbf{k}_1\hat{U}_{\mathbf{k}_1}\hat{U}_{\mathbf{k}_2}\sum_{\mathbf{k}_{\mathbf{n}}\neq 0}\hat{G}'_{\mathbf{k}_{\mathbf{n}}}\sum_{\mathbf{M}_1}\delta_{\mathbf{k}_1-\mathbf{k}_{\mathbf{n}}+\mathbf{M}_1}\sum_{\mathbf{M}_2}\delta_{\mathbf{k}_2+\mathbf{k}_{\mathbf{n}}+\mathbf{M}_2}.
\end{aligned} \tag{A6}$$

Here

$$\delta_{\mathbf{k}} = \begin{cases} 1 & \text{if } \mathbf{k}=0 \\ 0 & \text{if } \mathbf{k}\neq 0 \end{cases} \tag{A7}$$

is the Kronecker delta function and $\mathbf{M}_1,\mathbf{M}_2$ are triplets of multiples of the number of gridpoints in each dimension, as in Eq. (25). We have made use of the identity

$$\sum_{\mathbf{r}_{\mathbf{n}}} e^{i(\mathbf{k}-\mathbf{k}_{\mathbf{n}})\cdot\mathbf{r}_{\mathbf{n}}} = \sum_{\mathbf{M}}\delta_{\mathbf{k}-\mathbf{k}_{\mathbf{n}+\mathbf{M}}},$$

where the first sum is over all gridpoints, and the second is over all triplets of multiples of the number of gridpoints in each dimension.

Similarly,

$$\begin{aligned}
&\hat{\mathbf{E}}_{\mathrm{reciprocal}}(\mathbf{k}_1,\mathbf{k}_2) \\
&= -\frac{1}{V}\sum_{\mathbf{k}\neq 0} i\mathbf{k}\hat{G}_{\mathbf{k}}\left[\int_V e^{i(\mathbf{k}-\mathbf{k}_1)\cdot\mathbf{r}_1}d^3r_1\right]\left[\int_V e^{i(\mathbf{k}+\mathbf{k}_2)\cdot\mathbf{r}_2}d^3r_2\right] = -V\sum_{\mathbf{k}\neq 0} i\mathbf{k}\hat{G}_{\mathbf{k}}\delta_{\mathbf{k}_1-\mathbf{k}}\delta_{\mathbf{k}+\mathbf{k}_2} = -Vi\mathbf{k}_1\hat{G}_{\mathbf{k}_1}\delta_{\mathbf{k}_1+\mathbf{k}_2}[1-\delta_{\mathbf{k}_1}].
\end{aligned} \tag{A8}$$

Since

Author complimentary copy. Redistribution subject to AIP license or copyright, see http://jcp.aip.org/jcp/copyright.jsp

$$\sum_{\mathbf{k}_1}\sum_{\mathbf{k}_2}|\hat{\mathbf{E}}_{\mathrm{P^3M}}(\mathbf{k}_1,\mathbf{k}_2)|^2 = V^2\sum_{\mathbf{k}_1}\sum_{\mathbf{k}_2}|\mathbf{k}_1|^2\hat{U}^2_{\mathbf{k}_1}\hat{U}^2_{\mathbf{k}_2}\sum_{\mathbf{k_n}\neq 0,\mathbf{k}'_{\mathbf{n}}\neq 0}\hat{G}'_{\mathbf{k_n}}\hat{G}'_{\mathbf{k}'_{\mathbf{n}}}\times\sum_{\mathbf{M}_1}\delta_{\mathbf{k}_1-\mathbf{k_{n+M}}_1}\sum_{\mathbf{M}_2}\delta_{\mathbf{k}_2+\mathbf{k_{n+M}}_2}\sum_{\mathbf{M}'_1}\delta_{\mathbf{k}_1-\mathbf{k_{n'+M}}'_1}\sum_{\mathbf{M}'_2}\delta_{\mathbf{k}_2+\mathbf{k_{n'+M}}'_2}$$
$$= V^2\sum_{\mathbf{k_n}\neq 0}(\hat{G}'_{\mathbf{k_n}})^2\left[\sum_{\mathbf{M}}|\mathbf{k_{n+M}}|^2\hat{U}^2_{\mathbf{k_{n+M}}}\right]\left[\sum_{\mathbf{M}}\hat{U}^2_{\mathbf{k_{n+M}}}\right], \tag{A9}$$

$$\sum_{\mathbf{k}_1}\sum_{\mathbf{k}_2}\hat{\mathbf{E}}_{\mathrm{P^3M}}(\mathbf{k}_1,\mathbf{k}_2)\cdot\hat{\mathbf{E}}^*_{\mathrm{reciprocal}}(\mathbf{k}_1,\mathbf{k}_2) = V^2\sum_{\mathbf{k}_1}\sum_{\mathbf{k}_2}|\mathbf{k}_1|^2\hat{U}_{\mathbf{k}_1}\hat{U}_{\mathbf{k}_2}\hat{G}_{\mathbf{k}_1}\delta_{\mathbf{k}_1+\mathbf{k}_2}[1-\delta_{\mathbf{k}_1}]\times\sum_{\mathbf{k_n}\neq 0}G'_{\mathbf{k_n}}\sum_{\mathbf{M}_1}\delta_{\mathbf{k}_1-\mathbf{k_{n+M}}_1}\sum_{\mathbf{M}_2}\delta_{\mathbf{k}_2+\mathbf{k_{n+M}}_2}$$
$$= V^2\sum_{\mathbf{k_n}\neq 0}\hat{G}'_{\mathbf{k_n}}\left[\sum_{M}|\mathbf{k_{n+M}}|^2\hat{U}^2_{\mathbf{k_{n+M}}}\hat{G}_{\mathbf{k_{n+M}}}\right], \tag{A10}$$

and

$$\sum_{\mathbf{k}_1}\sum_{\mathbf{k}_2}|\hat{\mathbf{E}}_{\mathrm{reciprocal}}(\mathbf{k}_1,\mathbf{k}_2)|^2 = V^2\sum_{\mathbf{k}\neq 0}\hat{G}^2_{\mathbf{k}}|\mathbf{k}|^2, \tag{A11}$$

then

$$\chi^2_{\mathrm{P^3M}}V^{2/3} = \frac{1}{V^2}\sum_{\mathbf{k}_1}\sum_{\mathbf{k}_2}|\hat{\mathbf{E}}_{\mathrm{P^3M}}(\mathbf{k}_1,\mathbf{k}_2)|^2 - \frac{1}{V^2}\sum_{\mathbf{k}_1}\sum_{\mathbf{k}_2}\hat{\mathbf{E}}_{\mathrm{P^3M}}(\mathbf{k}_1,\mathbf{k}_2)\cdot\hat{\mathbf{E}}^*_{\mathrm{reciprocal}}(\mathbf{k}_1,\mathbf{k}_2) - \frac{1}{V^2}\sum_{\mathbf{k}_1}\sum_{\mathbf{k}_2}\hat{\mathbf{E}}^*_{\mathrm{P^3M}}(\mathbf{k}_1,\mathbf{k}_2)\cdot\hat{\mathbf{E}}_{\mathrm{reciprocal}}(\mathbf{k}_1,\mathbf{k}_2)$$
$$+\sum_{\mathbf{k}_1}\sum_{\mathbf{k}_2}|\hat{\mathbf{E}}_{\mathrm{reciprocal}}(\mathbf{k}_1,\mathbf{k}_2)|^2$$
$$= \sum_{\mathbf{k_n}\neq 0}(\hat{G}'_{\mathbf{k_n}})^2\left[\sum_{\mathbf{M}}|\mathbf{k_{n+M}}|^2\hat{U}^2_{\mathbf{k_{n+M}}}\right]\left[\sum_{\mathbf{M}}\hat{U}^2_{\mathbf{k_{n+M}}}\right] - 2\sum_{\mathbf{k_n}\neq 0}\hat{G}'_{\mathbf{k_n}}\left[\sum_{M}|\mathbf{k_{n+M}}|^2\hat{U}^2_{\mathbf{k_{n+M}}}\hat{G}_{\mathbf{k_{n+M}}}\right] + \sum_{\mathbf{k}\neq 0}\hat{G}^2_{\mathbf{k}}|\mathbf{k}|^2. \tag{A12}$$

Setting $\partial\chi^2_{\mathrm{P^3M}}/\partial\hat{G}'_{\mathbf{k_n}}=0$ gives Eq. (21),

$$\hat{G}'_{\mathbf{k_n}} = \frac{\Sigma_{\mathbf{M}}\hat{U}^2_{\mathbf{k_{n+M}}}\hat{G}_{\mathbf{k_{n+M}}}|\mathbf{k_{n+M}}|^2}{[\Sigma_{\mathbf{M}}\hat{U}^2_{\mathbf{k_{n+M}}}][\Sigma_{\mathbf{M}}\hat{U}^2_{\mathbf{k_{n+M}}}|\mathbf{k_{n+M}}|^2]}. \tag{A13}$$

Slightly different expressions may be derived for the case of differentiation on the reciprocal-space mesh, where the field is determined by multiplying the reciprocal-space mesh-based potential by $i\mathbf{k_n}$.

$$\mathbf{E}_{\mathrm{P^3M}}(\mathbf{r}_1,\mathbf{r}_2) = \sum_{\mathbf{r}'_{\mathbf{n}}}W(\mathbf{r}_1-\mathbf{r}'_{\mathbf{n}})\frac{1}{V}\sum_{\mathbf{k_n}\neq 0}e^{i\mathbf{k_n}\cdot\mathbf{r}'_{\mathbf{n}}}(-i\mathbf{k_n})\hat{G}'_{\mathbf{k_n}}\sum_{\mathbf{r_n}}e^{-i\mathbf{k_n}\cdot\mathbf{r_n}}W(\mathbf{r_n}-\mathbf{r}_2). \tag{A14}$$

Therefore,

$$\hat{\mathbf{E}}_{\mathrm{P^3M}}(\mathbf{k}_1,\mathbf{k}_2) = -\frac{1}{V}\sum_{\mathbf{r}'_{\mathbf{n}}}\left[\int_V W(\mathbf{r}_1-\mathbf{r}'_{\mathbf{n}})e^{-i\mathbf{k}_1\cdot\mathbf{r}_1}d^3r_1\right]\sum_{\mathbf{k_n}\neq 0}e^{i\mathbf{k_n}\cdot\mathbf{r}'_{\mathbf{n}}}i\mathbf{k_n}\hat{G}'_{\mathbf{k_n}}\sum_{\mathbf{r_n}}e^{-i\mathbf{k_n}\cdot\mathbf{r_n}}\times\left[\int_V W(\mathbf{r_n}-\mathbf{r}_2)e^{-i\mathbf{k}_2\cdot\mathbf{r}_2}d^3r_2\right]$$
$$= -\frac{1}{V}[\hat{W}_{\mathbf{k}_1}e^{-i\mathbf{k}_1\cdot\mathbf{r}'_{\mathbf{n}}}]\sum_{\mathbf{k_n}\neq 0}e^{i\mathbf{k_n}\cdot\mathbf{r}'_{\mathbf{n}}}i\mathbf{k_n}\hat{G}'_{\mathbf{k_n}}\sum_{\mathbf{r_n}}e^{-i\mathbf{k_n}\cdot\mathbf{r_n}}[\hat{W}_{\mathbf{k}_2}e^{-i\mathbf{k}_2\cdot\mathbf{r_n}}]$$
$$= -\frac{1}{V}\hat{W}_{\mathbf{k}_1}\hat{W}_{\mathbf{k}_2}\sum_{\mathbf{k_n}\neq 0}i\mathbf{k_n}\hat{G}'_{\mathbf{k_n}}\left[\sum_{\mathbf{r}'_{\mathbf{n}}}e^{-i(\mathbf{k}_1-\mathbf{k_n})\cdot\mathbf{r}'_{\mathbf{n}}}\right]\left[\sum_{\mathbf{r_n}}e^{-i(\mathbf{k_n}+\mathbf{k}_2)\cdot\mathbf{r_n}}\right]$$
$$= -V\hat{U}_{\mathbf{k}_1}\hat{U}_{\mathbf{k}_2}\sum_{\mathbf{k_n}\neq 0}i\mathbf{k_n}\hat{G}'_{\mathbf{k_n}}\sum_{\mathbf{M}_1}\delta_{\mathbf{k}_1-\mathbf{k_{n+M}}_1}\sum_{\mathbf{M}_2}\delta_{\mathbf{k}_2+\mathbf{k_{n+M}}_2}, \tag{A15}$$

$$\sum_{\mathbf{k}_1}\sum_{\mathbf{k}_2}|\hat{\mathbf{E}}_{\mathrm{P^3M}}(\mathbf{k}_1,\mathbf{k}_2)|^2 = V^2\sum_{\mathbf{k}_1}\sum_{\mathbf{k}_2}\hat{U}^2_{\mathbf{k}_1}\hat{U}^2_{\mathbf{k}_2}\sum_{\mathbf{k_n}\neq 0,\mathbf{k}'_{\mathbf{n}}\neq 0}\mathbf{k_n}\cdot\mathbf{k}'_{\mathbf{n}}\hat{G}'_{\mathbf{k_n}}\hat{G}'_{\mathbf{k}'_{\mathbf{n}}}\times\sum_{\mathbf{M}_1}\delta_{\mathbf{k}_1-\mathbf{k_{n+M}}_1}\sum_{\mathbf{M}_2}\delta_{\mathbf{k}_2+\mathbf{k_{n+M}}_2}\sum_{\mathbf{M}'_1}\delta_{\mathbf{k}_1-\mathbf{k_{n'+M}}'_1}\sum_{\mathbf{M}'_2}\delta_{\mathbf{k}_2+\mathbf{k_{n'+M}}'_2}$$
$$= V^2\sum_{\mathbf{k_n}\neq 0}|\mathbf{k_n}|^2(\hat{G}'_{\mathbf{k_n}})^2\left[\sum_{\mathbf{M}}\hat{U}^2_{\mathbf{k_{n+M}}}\right]^2, \tag{A16}$$

Author complimentary copy. Redistribution subject to AIP license or copyright, see http://jcp.aip.org/jcp/copyright.jsp

$$\sum_{\mathbf{k}_1}\sum_{\mathbf{k}_2}\hat{\mathbf{E}}_{\mathrm{P^3M}}(\mathbf{k}_1,\mathbf{k}_2)\cdot\hat{\mathbf{E}}^{*}_{\mathrm{reciprocal}}(\mathbf{k}_1,\mathbf{k}_2)$$
$$= V^2\sum_{\mathbf{k}_1}\sum_{\mathbf{k}_2}\hat{U}_{\mathbf{k}_1}\hat{U}_{\mathbf{k}_2}\hat{G}_{\mathbf{k}_1}\delta_{\mathbf{k}_1+\mathbf{k}_2}[1-\delta_{\mathbf{k}_1}]$$
$$\times\sum_{\mathbf{k_n}\neq 0}\mathbf{k_n}\cdot\mathbf{k}_1\hat{G}'_{\mathbf{k_n}}\sum_{\mathbf{M}_1}\delta_{\mathbf{k}_1-\mathbf{k_{n+M}}_1}<\sum_{\mathbf{M}_2}\delta_{\mathbf{k}_2+\mathbf{k_{n+M}}_2}$$
$$= V^2\sum_{\mathbf{k_n}\neq 0}\hat{G}'_{\mathbf{k_n}}\left[\sum_{M}\mathbf{k_n}\cdot\mathbf{k_{n+M}}\hat{U}^2_{\mathbf{k_{n+M}}}\hat{G}_{\mathbf{k_{n+M}}}\right], \tag{A17}$$

and

$$\chi^2_{\mathrm{P^3M}}V^{2/3} = \sum_{\mathbf{k_n}\neq 0}|\mathbf{k_n}|^2(\hat{G}'_{\mathbf{k_n}})^2\left[\sum_{\mathbf{M}}\hat{U}^2_{\mathbf{k_{n+M}}}\right]^2$$
$$-2\sum_{\mathbf{k_n}\neq 0}\hat{G}'_{\mathbf{k_n}}\left[\sum_{M}\mathbf{k_n}\cdot\mathbf{k_{n+M}}\hat{U}^2_{\mathbf{k_{n+M}}}\hat{G}_{\mathbf{k_{n+M}}}\right]$$
$$+\sum_{\mathbf{k}\neq 0}\hat{G}^2_{\mathbf{k}}|\mathbf{k}|^2. \tag{A18}$$

Setting $\partial\chi^2_{\mathrm{P^3M}}/\partial\hat{G}'_{\mathbf{k}_n}=0$ gives Eq. (22),

$$\hat{\mathbf{G}}'_{\mathbf{k_n}} = \frac{\Sigma_{\mathbf{M}}\hat{U}^2_{\mathbf{k_{n+M}}}\hat{G}_{\mathbf{k_{n+M}}}\mathbf{k_n}\cdot\mathbf{k_{n+M}}}{[\Sigma_{\mathbf{M}}\hat{U}^2_{\mathbf{k_{n+M}}}]^2|\mathbf{k_n}|^2}. \tag{A19}$$

[1] M. P. Allen and D. J. Tildesley, *Computer Simulation of Liquids* (Clarendon, Oxford, 1987).
[2] D. J. Tobias, Curr. Opin. Struct. Biol. **11**, 253 (2001).
[3] D. A. C. Beck, R. S. Armen, and V. Daggett, Biochemistry **44**, 609 (2005).
[4] C. J. Fennell and J. D. Gezelter, J. Chem. Phys. **124**, 234104 (2006).
[5] D. M. York, W. T. Yang, H. Lee, T. A. Darden, and L. G. Pedersen, J. Am. Chem. Soc. **117**, 5001 (1995).
[6] T. E. Cheatham and B. R. Brooks, Theor. Chem. Acc. **99**, 279 (1998).
[7] T. E. Cheatham, Curr. Opin. Struct. Biol. **14**, 360 (2004).
[8] R. W. Hockney and J. W. Eastwood, *Computer Simulation Using Particles* (IOP, Bristol, 1988).
[9] T. A. Darden, D. York, and L. G. Pedersen, J. Chem. Phys. **98**, 10089 (1993).
[10] U. Essmann, L. Perera, M. L. Berkowitz, T. Darden, H. Lee, and L. G. Pedersen, J. Chem. Phys. **103**, 8577 (1995).
[11] A. Toukmaji, C. Sagui, J. Board, and T. Darden, J. Chem. Phys. **113**, 10913 (2000).
[12] R. Zhou, E. Harder, H. Xu, and B. J. Berne, J. Chem. Phys. **115**, 2348 (2001).
[13] Y. B. Shan, J. L. Klepeis, M. P. Eastwood, R. O. Dror, and D. E. Shaw, J. Chem. Phys. **122**, 054101 (2005).
[14] M. Deserno and C. Holm, J. Chem. Phys. **109**, 7678 (1998).
[15] M. Deserno and C. Holm, J. Chem. Phys. **109**, 7694 (1998).
[16] V. Ballenegger, J. J. Cerda, O. Lenz, and C. Holm, J. Chem. Phys. **128**, 034109 (2008).
[17] J. Kolafa and J. W. Perram, Mol. Simul. **9**, 351 (1992).
[18] H. J. C. Berendsen, J. R. Grigera, and T. P. Straatsma, J. Phys. Chem. **91**, 6269 (1987).
[19] D. Frenkel and B. Smit, *Understanding Molecular Simulation: From Algorithms to Applications*, 2nd ed. (Academic, San Diego, 2002).
[20] T. Schlick, *Molecular Modeling and Simulation: An Interdisciplinary Guide* (Springer, New York, 2000).
[21] M. Levitt, Nature (London) **8**, 392 (2001).
[22] Acc. Chem. Res. **35**, 321 (2002), special issue on molecular dynamics simulations of biomolecules, edited by M. Karplus.

Author complimentary copy. Redistribution subject to AIP license or copyright, see http://jcp.aip.org/jcp/copyright.jsp